Accurate Design of Triplet Microstrip Square Open-Loop Resonator Filters

Marin V. Nedelchev, Ilia G.Iliev

Abstract: **This paper proposes a method for calculation of the coupling coefficients between coupled resonators used in triplet and cascaded triplet filters. Closed form formulas for the coupling coefficients are derived. The new approach for analytical computing the coupling coefficient represents an advance in the synthesis flexibility and reduces the time for design. The theory presented in the paper is validated by practical realizations of both main types of triplet filters. Measured results, obtained by the design technique, are shown. The results show very good agreement between the theory and measurement.**

Keywords: Microstrip bandpass filter, Cross-coupled resonators, coupling coefficients.

I. INTRODUCTION

In the modern communication systems, high selectivity and low passband loss are the main requirements for the microstrip filters. Low passband loss increases the system sensitivity and the high selectivity decrease the guard interval between two channels in a communication system. A better spectrum efficiency is achieved. High filter selectivity requires high filter order and more resonators. Because of the low unloaded Q factor of the microstrip resonators, the passband loss increases. Both requirements become contradictory for cascaded microstrip filters. Filters satisfying the increased requirements are the cross-coupled filters. They have non-adjacent resonator coupling.

The simplest cross-coupled filters are the trisection filters, proposed in [1,2]. They have asymmetric characteristics and one transmission zero (TZ) out of the passband. Quadruplet filters with one cross-coupling produces a pair of TZs symmetrically around the passband. These sections may be the core of cascaded triplet (CT) or cascaded quadruplet (CQ) filters [3,4,5] shown respectively on Fig.1a and Fig.1b.

The microstrip filter synthesis includes calculating the coupling coefficients for a given approximation (a method for Chebyshev approximation is presented in [6,7]) and their realization. The theory of coupling for synchronously and asynchronously tuned resonators is given in [8,9].

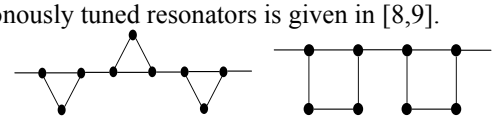

(a) (b)

Fig.1. Coupling and routing diagrams for cross-coupled filters. (a)Cascaded triplet. (b) Cascaded Quadruplet

Marin Veselinov Nedelchev and Ilia Georgiev Iliev –are with Dept. of Radiotechnic in Faculty of Communications and Communication Technologies in TU –Sofia, N8, Kliment Ohridski bul., 1700 Sofia, Bulgaria. E-mail: mnedelchev@tu-sofia.bg, igiliev@tu-sofia.bg.

A full-wave electromagnetic (EM) simulator is used to calculate the couplings in the papers [1,2,4,8], which is an expensive and time-consuming method. The use of EM simulator is not a flexible way for computation of the coupling coefficients. A design technique for synthesis of CQ filters without the use of EM simulator is given in [10]. A closed form formulas are derived for the basic couplings in the CQ filters.

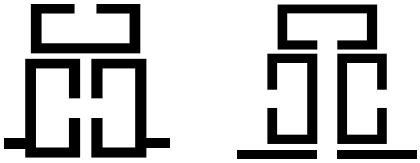

(a) (b)

Fig.2 Trisection filters. (a) realizes a TZ on the upper side of the passband. (b) realizes TZ on the lower side of the passband

In this paper is proposed a design technique for synthesis of trisection and CT filters (Fig.2) without full-wave EM simulator. Closed form formulas are derived for the coupling coefficients in the trisection and CT filters. Two filters are synthesized and measured. A comparison between the theoretical and the measured frequency responses is done and a good correlation is observed.

II. COUPLING COEFFICIENTS FOR DIFFERENT RESONATOR CONFIGURATIONS IN CT FILTERS.

The three microstrip square open-loop resonators in the trisection filter are asynchronously tuned. The self-resonant frequency of each resonator is f_{0i}, which is different from the filter's central frequency f_0. Resonators 1 and 3 are tuned on an equal frequency, i.e. $f = f_{01} = f_{03}$. For the microstrip square open-loop resonators their electrical length is $\theta_i \approx \frac{\pi}{2}$ *rad* for $f = f_{0i}$, *i=1,2,3*.

A. Electrical coupling

The cross-coupling between resonators 1 and 3, shown on Fig.2a, is electrical in nature, because the open ends of the lines are close and the electric fringe field is much stronger near the open ends. The coupled resonators are tuned on equal frequency and a closed form formula for the coupling coefficient is derived in [10] (Fig.3):

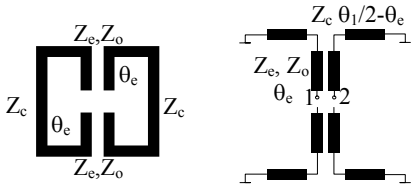

(a) (b)

Fig.3 Electric coupling. (a) Resonator topology (b) Equivalent scheme

$$k_e = \frac{1}{2b}\left(\frac{1}{Z_o}\frac{Z_o - Z_c tg\theta_e tg\left(\frac{\theta_1}{2}-\theta_e\right)}{Z_c tg\left(\frac{\theta_1}{2}-\theta_e\right) - Z_o tg\theta_e} - \frac{1}{Z_e}\frac{Z_e - Z_c tg\theta_e tg\left(\frac{\theta_1}{2}-\theta_e\right)}{Z_c tg\left(\frac{\theta_1}{2}-\theta_e\right) - Z_e tg\theta_e}\right) \quad (1),$$

where Z_c is the characteristic impedance of the transmission line,

Z_e и Z_o are the even and odd impedances of the coupled lines

θ_1 is the electrical length of the resonators

θ_e is the length of the coupled lines

b is the admittance slope of the resonators.

B. Magnetic coupling

The cross-coupling between resonators 1 and 3, shown on Fig.2b is magnetic in nature, because of the virtual ground in the middle of the resonator. A closed form formula for the coupling coefficient is derived in [10]. Figure 4 shows the resonator configuration and their equivalent scheme.

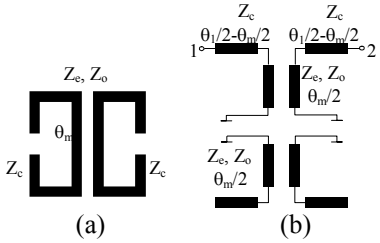

(a) (b)

Fig.4 Magnetic coupling. (a) Resonator topology (b) Equivalent scheme

$$k_m = \frac{1}{2bZ_c}\left(\frac{Z_c - Z_o tg\frac{\theta_m}{2}tg\frac{\theta_1-\theta_m}{2}}{Z_o tg\frac{\theta_m}{2} - Z_c tg\frac{\theta_1-\theta_m}{2}} - \frac{Z_c - Z_e tg\frac{\theta_m}{2}tg\frac{\theta_1-\theta_m}{2}}{Z_e tg\frac{\theta_m}{2} - Z_c tg\frac{\theta_1-\theta_m}{2}}\right), \quad (2)$$

where θ_m is the coupled line length.

C. Hybrid coupling.

Hybrid coupled resonators are shown on Fig.5a and Fig.6a. For this type of coupling none of the electromagnetic field components is much stronger than the other. It is important for these case that the resonators are asynchronously tuned. Their self-resonant frequencies are f_{01} и f_{02} and the electrical lengths are respectively θ_1 and θ_2 for the central frequency f_0.

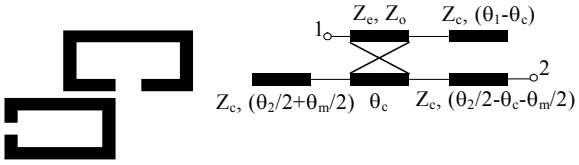

(a) (b)

Fig.5 Hybrid coupling 1 (a) Resonator topology (b) Equivalent scheme

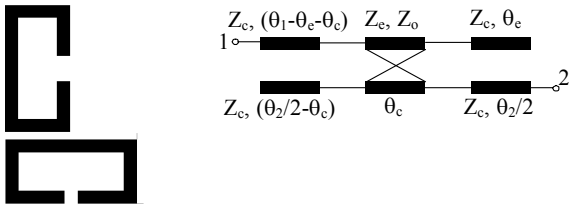

(a) (b)

Fig.6 Hybrid coupling 2. (a) Resonator topology (b) Equivalent scheme

For the hybrid coupling shown on Fig.5a and using the equivalent scheme on Fig.5b for the coupling coefficient is derived:

$$k_{hyb1} = \frac{y_{21}}{\sqrt{b_1 b_2}} \quad (3)$$

$$d_2 = \left[\frac{\cot g\theta_c}{w} - y_c tg\left(\frac{\theta_2}{2}+\frac{\theta_m}{2}\right)\right]\left[\frac{\cot g\theta_c}{w} + y_c tg\left(\theta_1-\theta_c\right)\right] - \frac{\csc^2\theta_c}{v^2}$$

$$y_{41} = j\frac{\csc\theta_c}{v} - j\frac{\csc\theta_c}{d_2 w}\left[\begin{array}{l} -\frac{\csc^2\theta_c}{vw} + \\ +\frac{\cot g\theta_c}{v}\left(\frac{\cot g\theta_c}{w} - y_c tg\left(\theta_1-\theta_c\right)\right)\end{array}\right] -$$

$$-j\frac{\cot g\theta_c}{d_2 v}\left[\begin{array}{l} -\frac{\cot g\theta_c \csc\theta_c}{v^2} + \\ +\frac{\csc\theta_c}{w}\left(\frac{\cot g\theta_c}{w} - y_c tg\left(\frac{\theta_2}{2}+\frac{\theta_m}{2}\right)\right)\end{array}\right]$$

$$y_{44} = j\frac{\cot g\theta_c}{w} - j\frac{\csc\theta_c}{d_2 w}\left[\begin{array}{l} -\frac{\cot g\theta_c \csc\theta_c}{v^2} + \\ +\frac{\csc\theta_c}{w}\left(\frac{\cot g\theta_c}{w} - y_c tg\left(\theta_1-\theta_c\right)\right)\end{array}\right] -$$

$$-j\frac{\cot g\theta_c}{d_2 v}\left[\begin{array}{l} -\frac{\csc^2\theta_c}{vw} + \\ +\frac{\cot g\theta_c}{v}\left(\frac{\cot g\theta_c}{w} - y_c tg\left(\frac{\theta_2}{2}+\frac{\theta_m}{2}\right)\right)\end{array}\right]$$

$$y_{21} = \left[jZ_c\frac{y_{44}}{y_{41}}\sin\left(\frac{\theta_2}{2}-\frac{\theta_m}{2}-\theta_c\right) - \frac{1}{y_{41}}\cos\left(\frac{\theta_2}{2}-\frac{\theta_m}{2}-\theta_c\right)\right]^{-1}$$

$$\frac{1}{v} = \frac{1}{2}\left(\frac{1}{Z_o}-\frac{1}{Z_e}\right) \quad \frac{1}{w} = \frac{1}{2}\left(\frac{1}{Z_e}+\frac{1}{Z_o}\right)$$

$$b_i = \frac{\pi}{2}y_c, \text{ за } i=1, 2.$$

For the hybrid coupling shown on Fig.6a and using the equivalent scheme on Fig.6b for the coupling coefficient is derived:

$$k_{hyb2} = \frac{y_{21}}{\sqrt{b_1 b_2}} \tag{4}$$

$$d_1 = \left[\frac{\cot g\theta_c}{w} - y_c tg\left(\frac{\theta_2}{2} - \theta_c\right)\right]\left[\frac{\cot g\theta_c}{w} + y_c tg\theta_e\right] - \frac{\csc^2\theta_c}{v^2}$$

$$y_{11} = -j\frac{\cot g\theta_c}{w} + j\frac{\cot g\theta_c}{d_1 v}\left[\begin{array}{l} -\dfrac{\csc^2\theta_c}{vw} + \\ +\dfrac{\cot g\theta_c}{v}\left(\dfrac{\cot g\theta_c}{w} - y_c tg\theta_e\right)\end{array}\right] +$$

$$+ j\frac{\csc\theta_c}{d_1 w}\left[\begin{array}{l} -\dfrac{\cot g\theta_c \csc\theta_c}{v^2} + \\ +\dfrac{\csc\theta_c}{w}\left(\dfrac{\cot g\theta_c}{w} - y_c tg\left(\dfrac{\theta_2}{2} - \theta_c\right)\right)\end{array}\right]$$

$$y_{41} = j\frac{\csc\theta_c}{v} - j\frac{\csc\theta_c}{d_1 w}\left[\begin{array}{l} -\dfrac{\csc^2\theta_c}{vw} + \\ +\dfrac{\cot g\theta_c}{v}\left(\dfrac{\cot g\theta_c}{w} - y_c tg\theta_e\right)\end{array}\right] -$$

$$- j\frac{\cot g\theta_c}{d_1 v}\left[\begin{array}{l} -\dfrac{\cot g\theta_c \csc\theta_c}{v^2} + \\ +\dfrac{\csc\theta_c}{w}\left(\dfrac{\cot g\theta_c}{w} - y_c tg\left(\dfrac{\theta_2}{2} - \theta_c\right)\right)\end{array}\right]$$

$$y_{14} = -y_{41}$$

$$y_{44} = j\frac{\cot g\theta_c}{w} - j\frac{\csc\theta_c}{d_1 w}\left[\begin{array}{l} -\dfrac{\cot g\theta_c \csc\theta_c}{v^2} + \\ +\dfrac{\csc\theta_c}{w}\left(\dfrac{\cot g\theta_c}{w} - y_c tg\theta_e\right)\end{array}\right] -$$

$$- j\frac{\cot g\theta_c}{d_1 v}\left[\begin{array}{l} -\dfrac{\csc^2\theta_c}{vw} + \\ +\dfrac{\cot g\theta_c}{v}\left(\dfrac{\cot g\theta_c}{w} - y_c tg\left(\dfrac{\theta_2}{2} - \theta_c\right)\right)\end{array}\right]$$

$$y_{21} = \left[\begin{array}{l} jZ_c \sin\dfrac{\theta_c}{2}\cos\left(\theta_1 - \theta_c - \theta_e\right)\dfrac{y_{44}}{y_{41}} - \\ -Z_c^2 \sin\dfrac{\theta_c}{2}\sin\left(\theta_1 - \theta_c - \theta_e\right)\left(\dfrac{y_{11}y_{44}}{y_{41}} + y_{14}\right) - \\ -\dfrac{1}{y_{41}}\cos\dfrac{\theta_2}{2}\cos\left(\theta_1 - \theta_c - \theta_e\right) - \\ -jZ_c \cos\dfrac{\theta_2}{2}\sin\left(\theta_1 - \theta_c - \theta_e\right)\dfrac{y_{11}}{y_{41}}\end{array}\right]^{-1}$$

$$\frac{1}{v} = \frac{1}{2}\left(\frac{1}{Z_o} - \frac{1}{Z_e}\right) \quad \frac{1}{w} = \frac{1}{2}\left(\frac{1}{Z_e} + \frac{1}{Z_o}\right)$$

$$b_i = \frac{\pi}{2} y_c \text{, за } i=1, 2$$

D. Tapped input/output electrical length

The tapped electrical length θ_t is found in [11] (Fig.7):

$$\theta_t = \sin^{-1}\left(\sqrt{\frac{G_a}{b_1 Q_e}}\right), \tag{5}$$

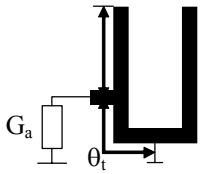

Fig.7. Tapped microstrip open-loop resonator

III. DESIGN TECHNIQUE FOR TRISECTION AND CT FILTERS.

1. Calculating the coupling matrix M and the external Q factor [6].
2. Finding the resonator parameters and the resonator self-resonant frequency. The main diagonal elements in the coupling matrix (M_{ii}) show the frequency deviation of each resonator. The angular self-resonant frequencies are the positive root of the equation:

$$\omega_{0i}^2 - M_{ii}\omega_0\omega_{0i} - \omega_0^2 = 0$$

Choosing the transmission line characteristic impedance Z_c and calculating the admittance slope parameter b_i.
3. Calculating the even and odd impedances of the coupled lines for different couplings Eqs. (1-4), the tapped input/output line length Eq. (5).
4. Computing the geometric dimensions of the filter for a given substrate.
5. Optimisation of the filter parameters.

IV. DESIGN EXAMPLES.

Two trisection filters are synthesized using the proposed formulas for the coupling coefficients. They are fabricated on a milling machine. The frequency responses are measured on HP8510C vector network analyzer. The analysis is performed using the electrical parameters of the filter. Both filters have central frequency $f_0=1.03GHz$, and fractional bandwidth $FBW=0.0776$. Both filters are fabricated on FR4 substrate with $\varepsilon_r = 4.5$, height $h = 1.5mm$ and $tg\delta = 0.019$. Considering the substrate parameters, high insertion loss is expected.

The first filter has a prescribed TZ on a frequency $f_0=900MHz$. The photograph of the filter is shown on fig.8. As can be seen the in-line couplings (1-2 and 2-3 resonators) are hybrid of I type (fig5). The cross coupling (1-3 resonator) is magnetic (fig.4).

Using Eqs. (2) and (3) are computed the even and odd mode impedances of the coupled lines for hybrid and magnetic coupling. The results are summarized in Table I.

TABLE1
ELECTRICAL PARAMETERS OF THE COUPLED LINES

	Even mode impedance Z_e [Ω]	Odd mode impedanc Z_o [Ω]	Electrical length of the coupled lines [deg]
Hybrid coupling of I type	74	33.78	30
Magnetic coupling	55.44	45.09	40

The coupling matrix is computed as:

$$M = \begin{bmatrix} 0 & 0.0945 & 0 & 0 & 0 \\ 0.0945 & 0.0094 & 0.0839 & 0.0382 & 0 \\ 0 & 0.0839 & -0.0369 & 0.0839 & 0 \\ 0 & 0.0382 & 0.0839 & 0.0094 & 0.0945 \\ 0 & 0 & 0 & 0.0945 & 0 \end{bmatrix}$$

The self-resonant frequencies are computed as follows: $f_{01}=f_{03}=1026MHz$ and $f_{02}=1045.5MHz$.

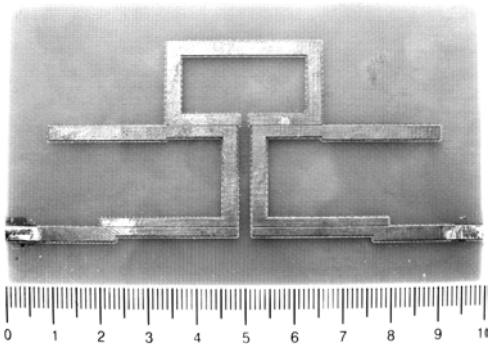

Fig.8 Photograph of the fabricated Filter1

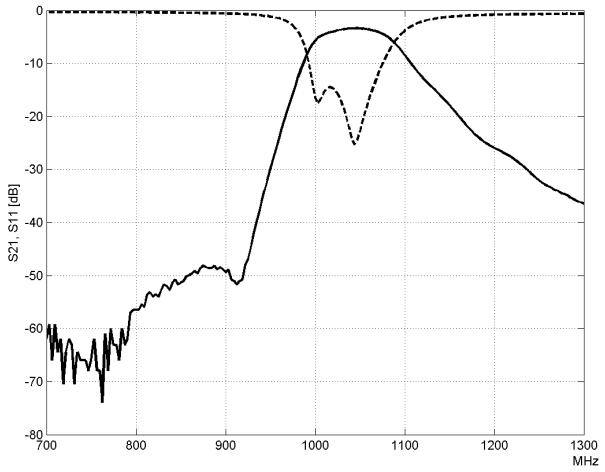

(a)

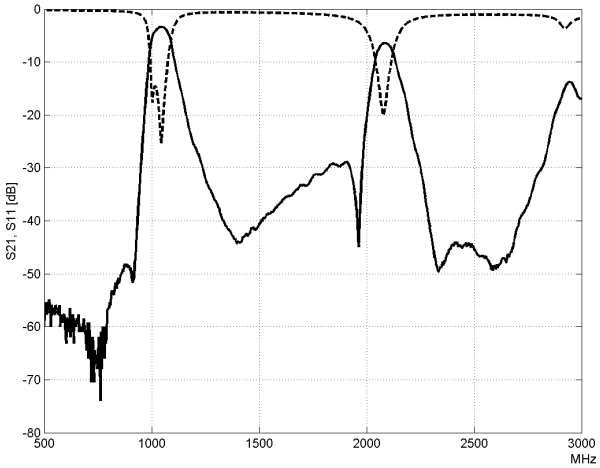

(b)

Fig.9.Filter 1 Measured frequency responses. (a) Insertion (solid line) and return (dashed line) loss. (b) Wideband frequency responses

The measured narrow and wideband frequency responses of the filter are shown on Fig.9. As can be seen from fig.9a the center frequency and the frequency responses of the filter are 10MHz higher than the prescribed 1030MHz. The measured bandwidth of the filter is 9MHz wider than the prescribed 80MHz. The attenuation in the passband is 3.4dB, mainly due to the dielectric losses in the substrate and the conductor losses. It is clearly seen that the return loss is better than -14.5dB and assures good matching of the filter with other devices connected to its input and output. The measured attenuation for the TZ frequency is better than 50dB and assures good suppression of neighbour channels in the lower stopband of the filter. The frequency of the TZ could be finely adjusted by tuning the cross coupling between the first and the third resonators. There is a parasitic TZ clearly seen in the wideband response on fig.9b. It is placed on 1400MHz. The close placement of the input and output transmission lines (fig.8) causes an extra TZ in the upper stopband of the filter. The frequency of this TZ could be adjusted by a tuning screw or a different distance between the input/output lines. The first parasitic passband is placed on the second harmonic of the central frequency. The filter is based on nearly halfwave resonators and such a result is expected.

B. The second filter has a prescribed TZ on a frequency $f_0=1150MHz$ (Fig.2a). The coupling matrix is computed as:

$$M = \begin{bmatrix} 0 & 0.0946 & 0 & 0 & 0 \\ 0.0946 & -0.0077 & 0.0861 & -0.0308 & 0 \\ 0 & 0.0861 & 0.0299 & 0.0861 & 0 \\ 0 & -0.0308 & 0.0861 & -0.0077 & 0.0946 \\ 0 & 0 & 0 & 0.0946 & 0 \end{bmatrix}$$

The self-resonant frequencies are computed as follows: $f_{01}=f_{03}=1034.9MHz$ and $f_{02}=1011.2MHz$. The photograph of the fabricated experimental filter is shown on fig.10. As can be clearly seen the in-line couplings (1-2 and 2-3 resonators) are hybrid of II type (fig.6). The cross coupling (1-3 resonator) is electric (fig.3). Using the derived Eqs. (1) and (4)

are computed the even and odd mode impedances of the coupled lines for hybrid and electric coupling. The results are shown in Table II.

TABLE II
ELECTRICAL PARAMETERS OF THE COUPLED LINES

	Even mode impedance Z_e [Ω]	Odd mode impedanc Z_o [Ω]	Electrical length of the coupled lines [deg]
Hybrid coupling of II type	77.75	32.15	30
Electrical coupling	57.52	43.46	10

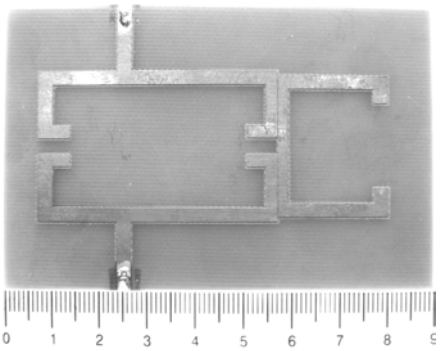

Fig.10. Photograph of the fabricated Filter2

The frequency responses of the filter are shown on Fig.11.

It is clearly seen from fig.11, that the measured responses are shifted with 10MHz in the higher frequencies. The measured central frequency of the filter is 1040MHz. The measured -3dB bandwidth is 70MHz and obviously is 10MHz narrower than the defined 80MHz. The minimum insertion loss is 3.8dB, and the attenuation on the frequency of the TZ is -44dB. The maximum value of the return loss is -10.4dB and assures good matching of the filter. The parasitic passband placed on the second harmonic of the center frequency of the filter is not well pronounced.

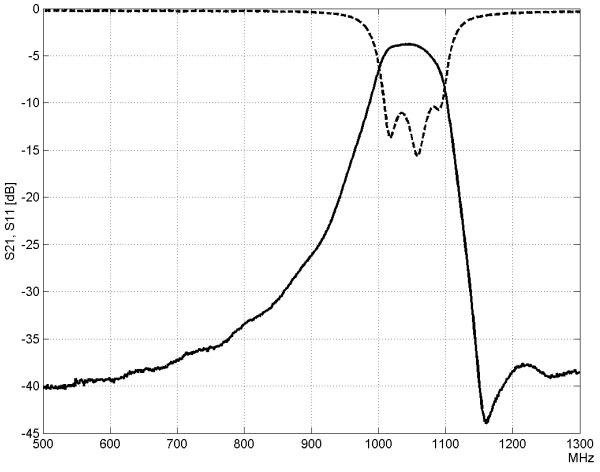

(a)

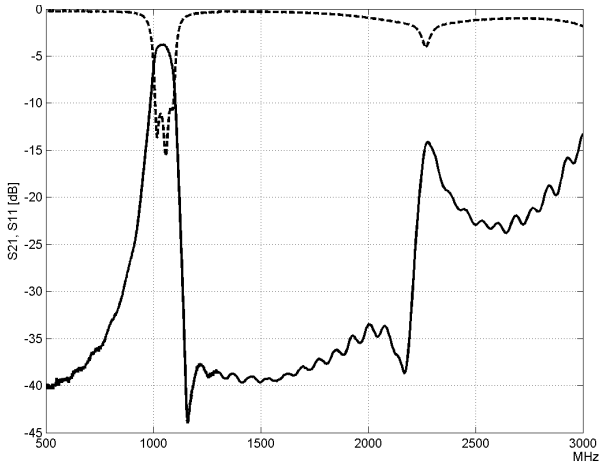

(b)

Fig.11.Filter 2 Measured frequency responses. (a) Transmission (solid line) and reflection (dashed line) coefficients. (b) Wideband frequency responses

V. CONCLUSION

The paper proposes a method for synthesis of trisection or CT filters. Closed-form formulas for different type of couplings are derived. The computation of the coupling coefficients is carried out without using a full-wave EM simulator. Measured results of two triplet filters are presented to validate the theory. There is a good agreement between the presented theory and the measurement results.

REFERENCES

[1] J.S.Hong, Lancaster, M, Microstrip Cross-Coupled Trisection Bandpass Filters with Asymmetric Frequency Characteristics, IEE Proc.-Microwave, Antennas, Propagation 146, Feb, 1999, pp.84-90

[2] Chih-Ming Tsai et al, Microstrip Trisection Cross-coupled Bandpass Filter with I-Shaped Resonator,

[3] Levy, R, Filters with Single Transmission zeros at Real or Imaginary Frequencies, IEEE Trans. On MTT-24, April 1976, pp.172-181

[4] J.S.Hong, Lancaster, M, Theory and Experiment of Novel Microstrip Slow-Wave Open Loop Resonator Filters, IEEE Trans. On MTT-45, Dec.1997, pp.2358-2365

[5] J.S.Hong, Lancaster, M, Cross-Coupled Microstrip Hairpin-Resonator Filters, IEEE Trans on MTT-46, Jan.1998, pp.118-122

[6] Cameron, R., et al, Synthesis of Advanced Microwave Filters Without Diagonal Cross-Coupling, IEEE Trans on MTT-49, Dec.2002, pp.2862-2871

[7] Cameron, R., Advanced Coupling Matrix Synthesis Techniques for Microwave Filters, IEEE Trans on MTT-50, Jan.2003, pp.1-10

[8] Rosenborg, U., Amari, S., Novel Coupling Schemes for Microwave Resonator Filters, IEEE Trans on MTT-49, Dec.2002, pp.2896-2902

[9] J.S.Hong, Couplings of Asynchronously Tuned Coupled Microwave Resonators, IEE Proc. Microwave, Antennas, Propagation 147, Oct. 2000, pp.354-358

[10] Iliev, I, Nedelchev, M, CAD of Cross-Coupled Miniaturized Hairpin Bandpass Filters, ICEST, Nis, Yugoslavia, 2002

[11] Wong, J, Microstrip Tapped-Line Filter Design, IEEE Trans on MTT-27, Jan.1979, pp.44-50